2 Days International Conference on Recent Innovations in Engineering, Science, Humanities and Management
Dev Samaj College for Women, Ferozepur, Panjab (India) (ICRIESHM-17)
18th -19th March 2017, www.conferenceworld.in ISBN: 978-93-86171-33-7

HEAVY ION INDUCED FISSION CROSS SECTION MEASUREMENT FOR $^{18}O+^{194}Pt$ SYSTEM

Ujalla

Assistant Professor, Physics Department, Dev Samaj College For Women, Ferozepur City, (India)

ABSTRACT

The study of heavy-ion induced fission fragment angular distribution continues to be a source of rich information as regards fission process in general and fission dynamics in particular. Considerable progress has been made towards understanding many features of the fission phenomenon. In the present work, we have measured the total fission cross section and anisotropy from the angular distribution for $^{18}O +^{194} Pt$ system at various beam energies.

Keywords: GPSC, SSBD

I INTRODUCTION

Nuclear Fission is the process by which nucleus split up in to two or more lighter nuclei either spontaneously or by the absorption of various particles like neutron,Proton, alpha-particles etc or gamma-rays.The fission process often produces free neutrons and photons(in the form of gamma-rays)and releases a very large amount of energy.The sum of the masses of the fragments is less than the original mass.The 'missing' mass has been converted into energy according to Einstein equation. The fission process was discovered on Dec 17 ,1938 by Otto Hahn and Fritz Strassman[1]. It Is an exothermic reaction which can release large amount of energy both as electromagnetic and kinetic energy of the fragments (heating the bulk material where fission takes place). Fission is a form of nuclear transmutation because the resulting fragments are not the same element as the original atom. The two nuclei produced are most often of comparable but slightly different sizes, typically with a mass ratio of products of about 3 to 2, for common fissile isotopes.

1.1. Requirements For Nuclear Reaction

There are following necesssary conditions which must be fulfilled if a reaction is to proceed.

Coulomb barrier- There is a coulomb repulsion between two interacting charged particles, called coulomb barrier. For a reaction to occur these particles must approach each other to within the order of nuclear dimension $=(10^{-15}m)$,or the kinetic energy of the incident particles must be compareable to or greater than the coulomb barrier.

Q-Value – For areaction with negative Q-Value ,a definite minimumkinetic energy is required for the reaction to takes place , which is called Threshold energy. For a positive Q-value reaction, there is no threshold enegy.

ISBN: 978-93-86171-33-7

Conservation laws – The certain physical quantities must be conserved before and after the reaction. The quantities conserved are the mass,energy,momentum,angular momentum,charge,number of nucleons,spin,parity and isospin. The parity is not conserved in weak interactions.

II HEAVY-ION INDUCED FISSION FRAGMENT ANGULAR DISTRIBUTION

Fission fragment angular distribution is an effective probe to understand the dynamics of heavy ion induced fission process .Through this study it has been possible to have insight regarding the evolution of the composite system formed during the interaction of two ions as it relaxes energy, mass, angular momentum and ultimately reaches the fully equilibrated compound nucleus. After the discovery of fission , Kramers[9] in 1940, pointed out that observation of significantly different values of fission probabilities as compared to the Bohr-Wheeler estimates would indicate the importance of nuclear dissipation not considered by them. It was generally believed after the compound nucleus was formed the transition time up to the saddle point and the subsequent fall time from the saddle to scission point were very fast to be of any consequence in influencing the fission process. In fact, almost all the low-energy fission data could be nicely explained the subsequent fall time from the saddle to scission point were very fast to be of any consequence using the saddle point model without incorporation of nuclear friction effects . However this was not capable of explaining the observation of a large number of pre-fission particle emitted in many heavy ion induced reactions which populated the compound nucleus at higher excitation energies between 50 and 100 Mev [3,4,6,7]. The presence of frictional forces effect not only the transient time from the equilibrium deformation to the saddle point but also the probability of passing over the saddle point. As a result of this the Bohr-Wheeler estimate of fission width gets reduced. At this stage the particle emission competes with fission decay and as a result of the additional delay time particle emission probability is considerably enhanced. This is the mechanism responsible for the observation of enhanced emission of pre-fission particles at these excitation energies. In fact particle decay can preceed fission both during the transition stage from equilibrium to saddle point and also later from saddle to scission point. Information regarding the dissipative forces can be gathered from a study of pre-fission particles. The emission of these pre-fission particles carrying away energy of the order of 10 Mev per particle from the compound nucleus excitation. energy ,has the net effect of cooling the residual compound nucleus formed at the saddle point According to the saddle point k_o^2 is given as $I_{eff}\,T/h^2$ where I_{eff} is the effective moment of inertia and T is the temperature at the saddle point .Due to pre-saddle emission of particles , the temperature is lowered and this in turn decreases the variance of the K-distribution (K_o^2).As the reduction in l of the compound nucleus due to the emission of these particle is more than the offset by the reduction in k_o^2 ,in the end there is an substantial increase in fission anisotropies A where A is defined as the $A= 1+<l^2>/k_o^2$ (as per the saddle –point model) where $<l^2>$ is the second moment of the compound nucleus spin distribution.

2.1. Models For Fission Fragment Angular Distributions

Fission fragment angular distributions are generally explained in terms of the transition state models. There are two types in general. One is SADDLE POINT MODEL and the other is SCISSION POINT MODEL [4, 6, 7]. The two

 ISBN: 978-93-86171-33-7

models depend on whether the characteristics of the ultimate fission fragments are decided at the saddle point or at the scission point. The touching spheroids represent the scission point and the other configuration which is more compact represents the saddle point. The compound nuclear angular momentum I, the body fixed symmetry axis for fission, the space fixed beam axis and the projection of I on the fissioning axis K are all shown in figure. The target spin effect has not been considered. The tilting angle Φ and the fragment emission angle with respect to the beam direction Θ are shown here. The saddle point model has had outstanding success in describing a large body of data mainly connected with lighter projectiles like nucleons, alphas. The scission point model has had success in describing some data for heavier projectiles beyond oxygen .According to saddle point model, the symmetry determined at the saddle point remain unaltered up to the scission point. The fission fragment angular distribution are controlled by fluctuations in the the orientations of of the fission decay axis with respect to the total angular momentum vector. The angular distributions are essentially determined at the saddle by the tilting of the disintegration axis with respect to the total angular momentum . This tilting is characterized by the r.m.s of the projection of I on the decay axis, K_0. The fission fragment angular distribution is given according to the saddle-point model as [2, 4 -11] (neglecting target and projectile spins and with I = l)

$$w(\theta) = \left(\frac{\pi}{k^2}\right) \sum_{l=0}^{l_{fus}} (2l+1)\, T_l \sum_{k=-l}^{l} [(2l+1)\left|d^l_{0,k}(\theta)\right|^2 * e^{\left(-\frac{K^2}{2K_0^2}\right)} / \sum_K e^{\left(-\frac{K^2}{2K_0^2}\right)}]$$

Where I_{fus} is the critical angular momentum for fusion (maximum) and $\left|d^l_{0,k}(\theta)\right|^2$ the rotational wave function. For large$l$, $\left|d^l_{0,k}(\theta)\right|^2 = [1/\pi]\,][(I+0.5)^2\,(\sin\theta)^2 - K^2]^{-1/2}$Here the variance of K distribution is

$K_0^2 = I_{eff}\ T/\hbar^2$ and $I/I_{eff} = I/I_{\perp} - I/I_{\parallel}$

where $I_{\perp}$ and $I_{\parallel}$ are the moments of inertia about an axis perpendicular to the symmetry axis and parallel to it. The saddle-point temperature T = $[E_x/a]^{1/2}$ where E_x, is the excitation energy at the saddle point, and a is the level density parameter.

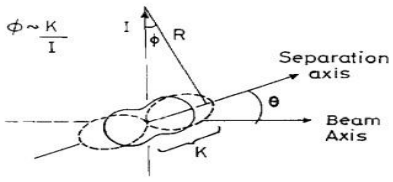

Figure 1: Fissioning system, as per the saddle point model and as per the scission model.

2.2. Anisotropy

ISBN: 978-93-86171-33-7

Experimentally it is well established that the fragments are emitted preferentially in the forward and backward directions with respect to the beam direction. Angular anisotropy is defined as the ratio of differential cross section of the fragments along the beam direction (W (180°) or W (0°)) to that in the perpendicular (W (90°)) direction. According to statistical saddle point model anisotropy is defined as

$A = W(180^0 \text{ or } 0^0) / W(90^0) \approx 1 + [\langle l^2 \rangle / 4K_0^2]$,

where $\langle l^2 \rangle$ is the second moment of compound nucleus spin distribution. The analysis of a data in case of many nucleon and light ion induced reactions were indeed found to be in good agreement with liquid drop model. The corresponding expression for angular distribution in the case of scission –point model is almost identical in form with K_0^2 replaced by sum of K_1^2 and $K_2^2$of the two fragments in this case.

2.3 Differential Cross-Section

The distribution in angle of emitted particles in a nuclear reaction can be described in terms of cross-section which is a function of angular coordinates. The cross-section which defines a distribution of emitted particles with respect to the solid angle is called differential cross-section.it is defined by $d\sigma/d\Omega$. Fission fragment angular distribution has been measured for $^{18}O + ^{194}Pt$ system with E_{lab} = 85 - 107 Mev using the differential cross-section expression which is given in section 4.

III EXPERIMENTAL SET -UP

The experiment was carried out in General Purpose Scattering Chamber (GPSC) at IUAC [13], New Delhi, using $^{16,18}O$ DC beam of energies in the range of 85-107 Mev. Self supporting target of Pt^{194} having a thickness around1.7mg/cm^2 was used for the measurement of the angular distribution of fission fragments. Single fission fragments were detected in the angular range of 54° to 168° in laboratory frame using two Si-detector telescopes and three ΔE-E gas- surface hybrid detectors.

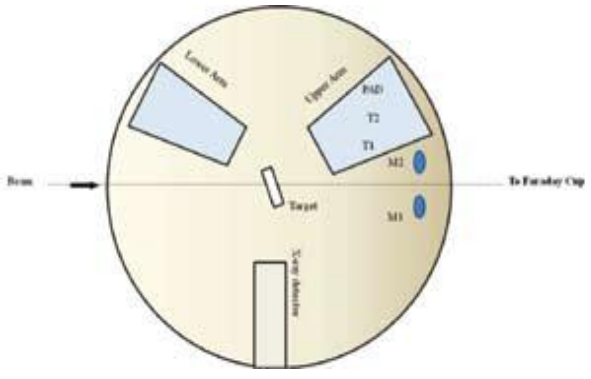

Figure 2: Experimental Layout

ISBN: 978-93-86171-33-7

The thickness of Silicon Surface Barrier Detector-E (T1, T2) was about 300 µm. The E detectors were backed by 10µm thick ΔE Si-Surface barrier detectors. The thickness of the E detectors in ΔE-E gas -surface barrier detectors (T3, T4, T5) was 100µm.The distances of the telescopes from the target were about 13.3 cm and the distances for ΔE-E gas-surface barrier hybrid detectors were 28.7, 27.6 and 28.5 cm respectively .Each detector had an angular coverage of about ±1°.The detectors (gas ΔE-E) were operated at about 100mbar gas pressure which correspond to an equivalent Silicon thickness of 2.5µm. Two monitors Si detectors (M1, M2) with 1mm collimator were kept at ±10° with respect to the beam at a distance of about 70cm from the target position to monitor Rutherford scattering .The relative solid angles of the telescopes were taken into account by measuring the data at overlapping angles. The SSBD telescope signal (ΔE) were processed through pre-amplifiers (142 IH) then amplifier (Ortec 571) and E signal of hybrid gas detectors processed through pre-amplifiers (Ortec 571,4417) then the dual sum signal of both the detectors was given to single channel analyzer(SCA 2037A) then these signal OR-ed using coincident unit. This OR-ed output signal was used as the trigger for the data acquisition system.

The online data were collected, event-wise for sufficient time period required for reasonable statistical accuracy, later analyzed using software CANDLE [14].Two-dimensional spectrum of DE versus energy of the particles reaching the E-detector was used to separate the fission fragments from quasi-elastic particles. As the fission fragments are very heavy and loose energy very fast , they get stooped in the first detector itself. However the scattered particle deposit very little energy in the first detector .In this way, the fission fragment can be easily separated from the scattered particles using the detector telescopes. Fig 3. shows the two dimensional spectra of versus ΔE for hybrid gas detector (T4) showing fission and quasi fission events for $^{18}O + ^{194}Pt$ at E_{cm}= 89.22Mev

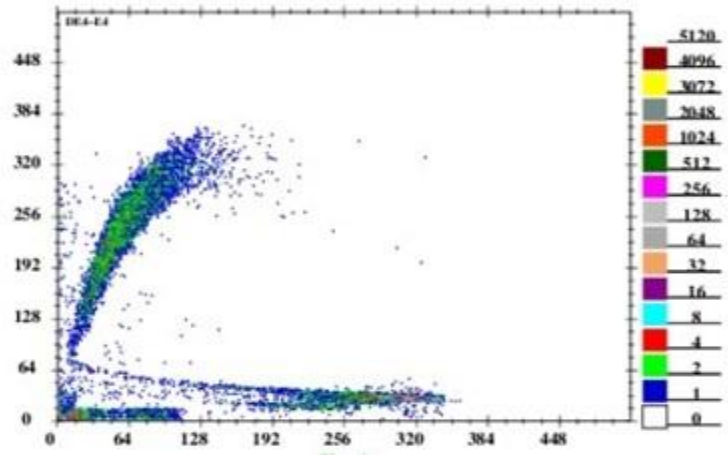

. Figure 3: A two dimensional spectra showing energy loss of particles in hybrid detector in $^{18}O+ ^{194}Pt$ at 97.5 Mev lab energy

3.1 Hybrid Detector Telescopes

ISBN: 978-93-86171-33-7

Hybrid telescopes, having combination of gas (ΔE) and silicon detectors has been used to study the angular distributions of fission fragments .The detector system can also be used to identify projectiles like fragments .These detector been developed for heavy ion detection particle identification in nuclear physics experiments in GPSC (General Purpose Scattering Chamber) facility at IUAC [13].ΔE–E identification technique is threshold dependent governed by the thickness of the ΔE detector. The 10mm thick detector is opaque to low energy heavy ions such as fission fragments and heavy projectiles. In such cases a gas detector is extremely useful since its thickness can be varied by simply adjusting the gas pressure and thus making its transmission type for low energy heavy ions.

3.1.1 Discription of Detector

It consist of a gas ionization chamber, operation in axial field geometry mode, followed by a silicon surface barrier detector (100μm) thick from Canberra. The ionization chamber is composed of three wires of diameter 1cm. The wire frames are cathode, a central anode frame ,and another cathode frame. The distance between adjacent wire frame is 10mm. All Wire frames are is 10mm. all the wire frame were made from gold plated tungsten wires of 20μm diameter stretched on a 3.2 mm thick printed circuit board .The separation between adjacent wire is 1mm. The cathodes are grounded whereas the anode operates in ionization region with atypical reduced field of about 2 V cm^{-1} $mbar^{-1}$ .The electrodes are housed inside cylindrical tube. The detector is operated with Isobutene gas at a pressure 10-200 mbar. Anode is used using in-house fabricated charge sensitive pre-amplifier of sensitivity of 90 mV/Mev (silicon equivalent) and the SSBD has a charge sensitive pre-amplifier of sensitivity 20 mv/Mev .for improved resolution; the pre- amplifier is placed next to the detector inside the vacuum chamber. In the detector set up for investigating the fission anisotropy of system $^{16, 18}O + {}^{194, 198}Pt$ .Three hybrid detector were placed at a distance of 30 cm from the target with angular separation of 12degree . Each detector had an angular coverage of about ± 1 degree. The detector was operated at 100 mbar gas pressure which corresponds to an equivalent silicon thickness of 2.5 mm. Two silicon telescopes were placed at other arm of GPSC .Both sets of telescopes yielded identical results in terms of cross section measurement.

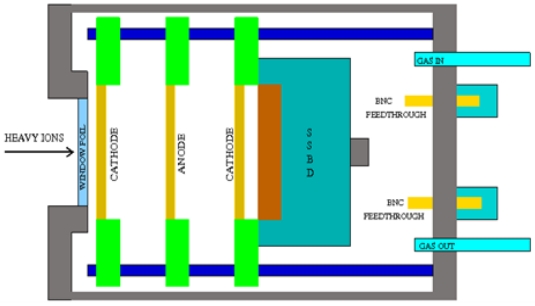

Figure 4: Schematic diagram of Hybrid Detector

IV DATA ANALYSIS AND RESULTS

ISBN: 978-93-86171-33-7

The measured fission fragment angular distributions were transformed from laboratory to centre of mass frame using Viola systematic for symmetric fission .The differential fission cross-section was calculated using the expression

$$\left(\frac{d\sigma}{d\Omega}\right)_{lab} = \frac{1}{2}\frac{y_{fiss}}{y_{mon}}\left(\frac{d\sigma}{d\Omega}\right)R\,\frac{\Omega_{mon}}{\Omega_{fiss}} \qquad -1$$

Where Y_{fiss} and Y_{mon} are the yields recorded by the fission detector and monitor (Rutherford) detector, respectively. Ω_{fiss} and Ω_{mon} are the solid angles subtended by the fission detector and monitor detector, respectively. $(d\sigma/d\Omega)_R$ is the differential Rutherford cross-section in the laboratory system. The Rutherford cross-section in laboratory frame can be written as

$$\left(\frac{d\sigma}{d\Omega}\right)R = 1.296(Z_pZ_t\ /E_{lab})^2\left[\frac{1}{(\sin\theta/2)^4} - 2(M_p/M_t)^2\right] \qquad -2$$

Where Zp, Zt and Mp and Mt are the atomic numbers and mass number of the projectile and target respectively. E_{lab} and θ are the energy of the incident particle and scattering angle of projectile-like particles in the laboratory frame of reference respectively.

The online data were collected and analyzed using software CANDLE. In order to calculate $(d\sigma/d\Omega)$, firstly fission yield Y_{fiss} was measured by applying gate on fission events in 2-D spectrum of DE verses E, the energy of the particle reaching the E detector and counting the area of that portion to which gate is applied. Fission yield detected by three detector telescopes T3, T4, T5 from 2-D DE3~E3 , DE4~E4 , DE5~E5 spectrum were measured .Similarly YM_2 ,YM_1 monitor counts were measured from the 1-D spectrum by applying gate and counting the area of that portion. YM was calculated by averaging the counts of YM_1, YM_2. For symmetric fission fragments, detector telescopes must be at same solid angle. For this purpose solid angle normalization was done. For normalization of the detector, θ_{lab} of T3 detector was kept fixed. However T4, T5 were kept at same angle as that of T3 from incident beam. For this set up fission yield and monitor yield were measured from the 2-D and 1-D spectrum in similar manner as we done in previous one. Then using expression

$$\frac{\Omega_{d1}}{\Omega_{d2}} = \frac{Y_{fiss(d1)}}{Y_{fiss(d2)}} * \frac{Y_{mon(d2)}}{Y_{mon(d1)}}$$

where d1 and d2 in subscript are used for any two fission detectors and monitor. Fission solid angle ratio of two detectors T3, T4 and T3, T5 were calculated, then Y_{fiss} detected by T3, T4, T5 detector were multiplied by 1 , 1.019 ,1.299.

4.1 Calculated values are

$\Omega_{T3}/\Omega_{T4} = 1.019$, $\Omega_{T3}/\Omega_{T5} = 1.299$

ISBN: 978-93-86171-33-7

Solid angle subtended by monitor and fission detector was calculated using the expression

$$d\Omega = \frac{dA}{r^2} = \frac{\pi R^2}{r^2}$$

where r is the distance between the target and monitor or fission detector. R is the radius of monitor or fission detector. The transformations from lab to center of mass system were done by using the expressions $\left(\frac{d\sigma}{d\Omega}\right)_{CM} = J_\sigma \left(\frac{d\sigma}{d\Omega}\right)_{lab}$, $\theta_{CM} = J_\theta \theta_{lab}$ and $E_{CM} = \frac{A_T}{A_T + A_P} * E_{lab}$ Where J_σ and J_θ are jacobian corresponding to cross-section and angle. A_T and A_P are mass number of target and projectile nuclei. Plots were generated between differential cross-section and the angle (between detector telescope and incident beam) in the center of mass system at different incident energies. The angular distributions were fitted to Legendre polynomial up to the second order and also extrapolation was done starting from 90^0 to 180^0. From the plot area under the curve was measured. The total fission cross-section can be written as

$$\sigma_f = 2\pi \int (d\sigma/d\Omega)_{CM} \sin\theta \; d\theta$$

and also by using the values of angular distributions at 180^0 and 90^0 from the plot, the anisotropy in angular distribution can be calculated by the expression

A= W (180^0 or 0^0) / W (90^0)

V CALCULATIONS

$^{18}O + ^{194}Pt$ @ E_{lab}=85 Mev, E_{cm} =77.77 Mev

YM = $\sqrt{YM1 * YM2}$

θ_{lab}	Y_{fiss}	YM2	YM1	Y_{fiss}/YM	θ_{cm}	$(d\sigma/d\Omega)_{cm}$ mb/str	$\pm\delta(d\sigma/d\Omega)_{cm}$ mb/str
78	2180	1519807	962660	0.0018	90.31	1.70	0.036
88	903	853349	600928	0.0033	100.69	1.65	0.065
90	2074	1500224	962421	0.0017	102.62	1.62	0.033
102	2414	1514704	970056	0.0203	114.38	2.22	0.044
112	1782	862236	553600	0.0237	123.72	3.16	0.075
124	1856	865779	556658	0.0232	134.75	3.71	0.074
144	2022	797679	528886	0.0031	151.37	4.55	0.101
156	2336	814630	527163	0.0035	161.11	4.94	0.102
168	3319	821704	524330	0.0505	170.61	7.72	0.082

ISBN: 978-93-86171-33-7

$^{18}O + ^{194}Pt$ @ E_{lab}=90 Mev ,E_{cm}= 82.35 Mev

θ_{lab}	Y_{fiss}	YM2	YM1	Y_{fiss}/YM	θ_{cm}	$(d\sigma/d\Omega)_{cm}$ mb/str	$\pm\delta(d\sigma/d\Omega)_{cm}$ mb/str
78	1926	369920	283306	0.0059	91.79	5.13	0.11
88	1747	335237	259957	0.0059	101.05	5.43	0.12
90	1960	369254	284233	0.0060	102.98	5.11	0.11
100	1361	231398	177867	0.0067	112.78	6.76	0.18
112	1782	281827	218050	0.0071	124.00	7.93	0.19
124	1922	281992	220831	0.0077	134.82	11.92	0.25
144	2267	277989	217502	0.0081	151.60	12.22	0.25
156	2797	272935	217537	0.0102	161.28	14.43	0.26
168	4175	277081	219164	0.0150	170.69	23.61	0.22

$^{18}O + ^{194}Pt$ @ E_{lab}=107 Mev , E_{cm} =97.70 Mev

θ_{lab}	Y_{fiss}	YM2	YM1	Y_{fiss}/YM	θ_{cm}	$(d\sigma/d\Omega)_{cm}$ mb/str	$\pm\delta(d\sigma/d\Omega)_{cm}$ mb/str
78	5791	121489	112490	0.045	91.92	29.87	0.377
90	5513	121713	114160	0.046	104.30	28.46	0.389
100	9654	426069	279177	0.027	113.96	29.50	0.175
102	6908	122273	112109	0.059	115.93	30.67	0.577
112	8208	266015	173076	0.038	125.22	34.84	0.187
124	9314	266766	170882	0.043	135.75	40.76	0.360
144	14641	331237	216150	0.054	152.28	50.79	0.450
156	18759	330099	211873	0.070	161.76	66.35	0.300
168	30895	332511	215044	0.115	170.91	119.76	0.410

VI OBSERVATIONS

Measured fission cross-sections for $^{18}O + ^{194}Pt$ system

E_{lab} (Mev)	$E_{cm}(Mev)$	σ_{fiss} (mb)	$\pm error$ (mb)
85.0	77.77	100.5	3.7

ISBN: 978-93-86171-33-7

90.0	82.35	248.6	9.15
107.0	97.90	1074.9	21.1

Measured anisotropy in angular distribution for $^{18}O + ^{194}Pt$ system

E_{cm} (Mev)	Anisotropy (A)	$\pm\delta A$ (error)
77.77	4.35	0.087
82.35	4.28	0.085
97.90	5.03	0.100

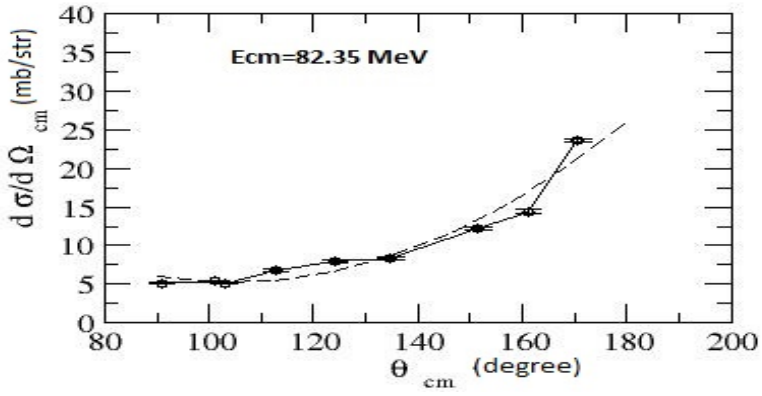

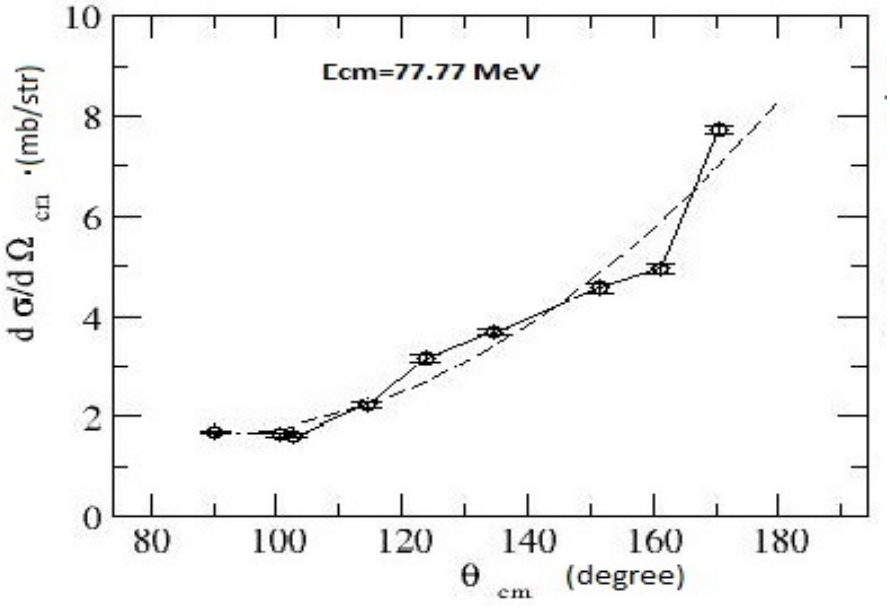

ISBN: 978-93-86171-33-7

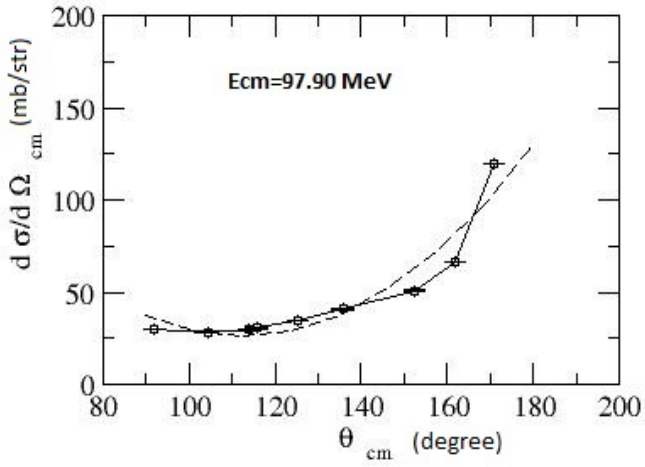

Figure5: Fission fragment angular distributions at different beam energies for $^{18}O + ^{194}Pt$ Dotted lines are the fits using Lagendre Polynomial (solid circles shows error in angular distribution.)

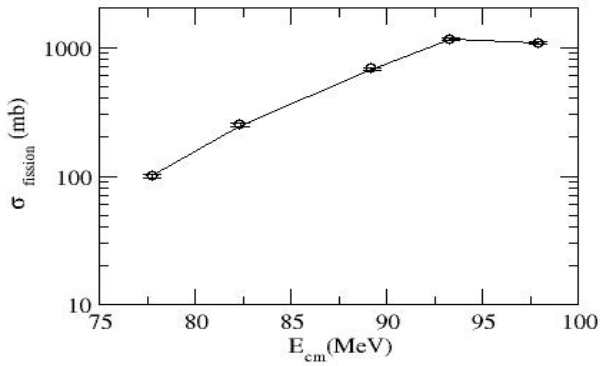

Figure6: fission cross section for $^{18}O + ^{194}Pt$ at different beam energies (solid circles shows error in fission cross section values).

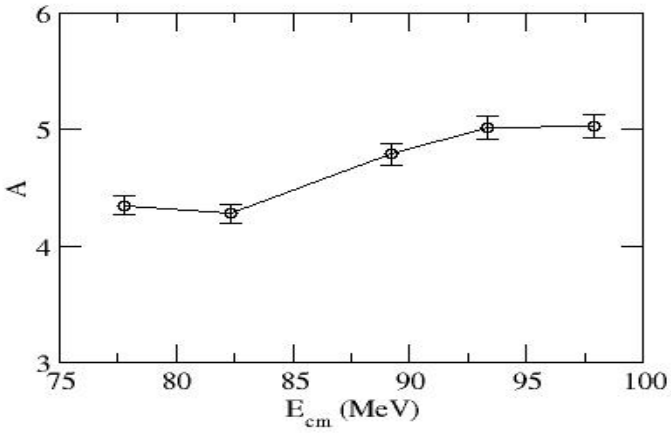

ISBN: 978-93-86171-33-7

Figure7: Anisotropy in angular distribution at different beam energies.

VII CONCLUSION

From the angular distribution plot, we have measured the total fission cross section and also calculated the anisotropy in angular distribution at various beam energies. Finally, from anisotropy we can obtain $< l^2 >$, the second moment of compound nucleus spin distribution.

REFERENCES

1. R.R. Roy and B.P. Nigam.
2. S. Kailas, R. Vandenbosch, A. Charlop, S.J. Luke, D. Prindle and S. Van Verst, Phys. Rev. C 42 (1990) 2239.
3. R.Vandenbosch, Nucl. Phys. A 502 (1989) 1c.
4. J.A. Wheeler, in: Fast Neutron Physics, eds. J.B. Marion and J.L. Fowler (Wiley-Interscience, New York, 1963).
5. W.Q. Shen, J. Albinski, A. Gobbi, S. Gralla, K.D. Hildenbrand, N. Herrmann, J. Kuzminski, W.F.J. Muller, H. Stelzer, J. Toke, B.B. Back, S. Bjornholm and S.P. Sorensen, Phys. Rev. C 36 (1987) 115.
6. R. Freifelder, M. Prakash and J.M. Alexander, Phys. Rep. 133 (1986) 315
7. L.C. Vaz and J.M. Alexander, Phys. Rep. 97 (1983) 1.
8. H.A. Kramers, Physica 7 (1940) 284.
9. N. Bohr and J.A. Wheeler, Phys. Rev. 56 (1939) 426.
10. U.L. Businaro and S. Gallone, Nuovo Cimento 5 (1957) 315; K.T.R. Davies and A.J. Sierk, Phys. Rev. C 31 (1985) 915; M. Abe, KEK preprint 86-26, KEK TH-28 (1986).
11. V.S. Ramamurthy and S.S. Kapoor, Proc. lnt. Conf. on Nucl. Phys., Harrogate, UK, eds J.L. Durell, J.M. Irvine and G.C. Morrison, IOP Conf. Proc. No. 86 (Institute of Physics, Bristol, 1986) Vol. 1, p. 292.
12. A.Jhingan. S. Kalkal, Varinderjit singh, R. Sandal, B. R. Behera. S. K. Mandal, P. Sugathan, Proc. Of the DAE Symp. On Nucl. Phys. 56, 1040 (2011).
13. Rohit Sandal, B.R. Behera , V. singh, M.Kaur, S.Mandal, D. Siwal, S.Goyal, E. Prasad, P.sugathan, A.Jhigan, A. Saxena Proc. DAE Symp. Nucl. Phys, Vol 57, 534 (2012).
14. E. T. Subramanian, B. P. Ajith kumar , and R. K. Bhowmik